45p

SURFACE TEMPERATURE VARIATIONS DURING THE LUNAR NIGHTTIME

by

Bruce C. Murray
Robert L. Wildey

Division of Geological Sciences
California Institute of Technology
Pasadena, California

May 17, 1963

(Submitted to the Astrophysical Journal)

Contribution number 1173 of the Division of Geological Sciences, California Institute of Technology, Pasadena, California.

CONTENTS

I INTRODUCTION

The thermal emission of the Moon observed through the 8-14 micron window in the earth's atmosphere provided evidence of the enormous diurnal surface temperature variation on the moon even to the earliest workers in the field of infrared photometry (Rosse, 1869; Very, 1898). The eclipse cooling observations of Pettit and Nicholson (1930) constituted the first direct evidence of the unexpectedly high thermal insulation which characterizes the outermost layer of the Moon and which set off speculation regarding the nature and subsurface structure of these strange surface materials. More recently Shorthill, Borough, and Conley (1960), followed by Sinton (1960), made the major discovery that at least some bright rayed craters cool more slowly during an eclipse than do the surrounding areas. This discovery of locally more conductive surface deposits was the first definite evidence of horizontal variations in the bulk physical properties of the lunar surface (as distinguished from the variations in strictly surface properties like albedo and color) and might be regarded as the beginning of real geophysical exploration of the lunar surface.

During 1961, an effort was initiated at Caltech to exploit, for astronomical purposes, the high instrumental sensitivity potentially available with newly-developed photoconductive detectors sensitive out to 14 microns and beyond. A primary goal was, and continues to be, the investigation of 8-14 μ thermal emission of the Moon, particularly during the lunar nighttime when important vertical as well as horizontal variations in thermal properties may be evidenced. A preliminary report of our

8-14 micron emission observations into the first 160 hours of the lunar nighttime appeared recently as a brief note (Murray and Wildey, 1963). In the present paper those observations are described in full and the evidence of both horizontal and vertical variations in thermal properties of the lunar surface discussed. Also it is pointed out that these new thermal observations, along with recent radar observations, are strongly suggestive of surface redistribution processes presently active on the lunar surface.

II COLLECTION AND REDUCTION OF OBSERVATIONS

a) Equipment and Site

The equipment and site used for the collection of the lunar observations are described in detail by Westphal, Murray, and Martz (1963, in press). The basic element of the photometric system is a mercury-doped germanium photoconductive cell* at the apex of a conical cavity which is maintained at liquid hydrogen temperature ($\sim 20^{\circ}K$). An f/15 (3.8°) beam of radiation from the primary mirror is directed into the cold cavity by a Fabry lens constructed of barium floride which produces a real image of the primary mirror on the cell. An interference filter within the cavity, combined with the intrinsic cut off of long-wavelengths by the cell sensitivity, restricts the effective photon flux of the f/15 beam to the interval 8 - 14 microns as shown in Figure 1. Thus the total "background" radiation falling onto the photoconductive surface from the "hot" atmosphere, telescope components and surroundings, (together with the consequent photon noise) is restricted to a tiny fraction of that which would impinge on, for instance, a blackened thermal detector operated at ambient temperature. The doped-germanium photoconductor mounted in this fashion has a noise-equivalent-power approaching 2×10^{-12} watts, i.e., about 100 times smaller than that of a good thermal detector operated under normal circumstances. Further sophistication of equipment eventually may lead to a noise-equivalent power approaching 10^{-14} watts.

*Manufactured by Texas Instruments, Inc.

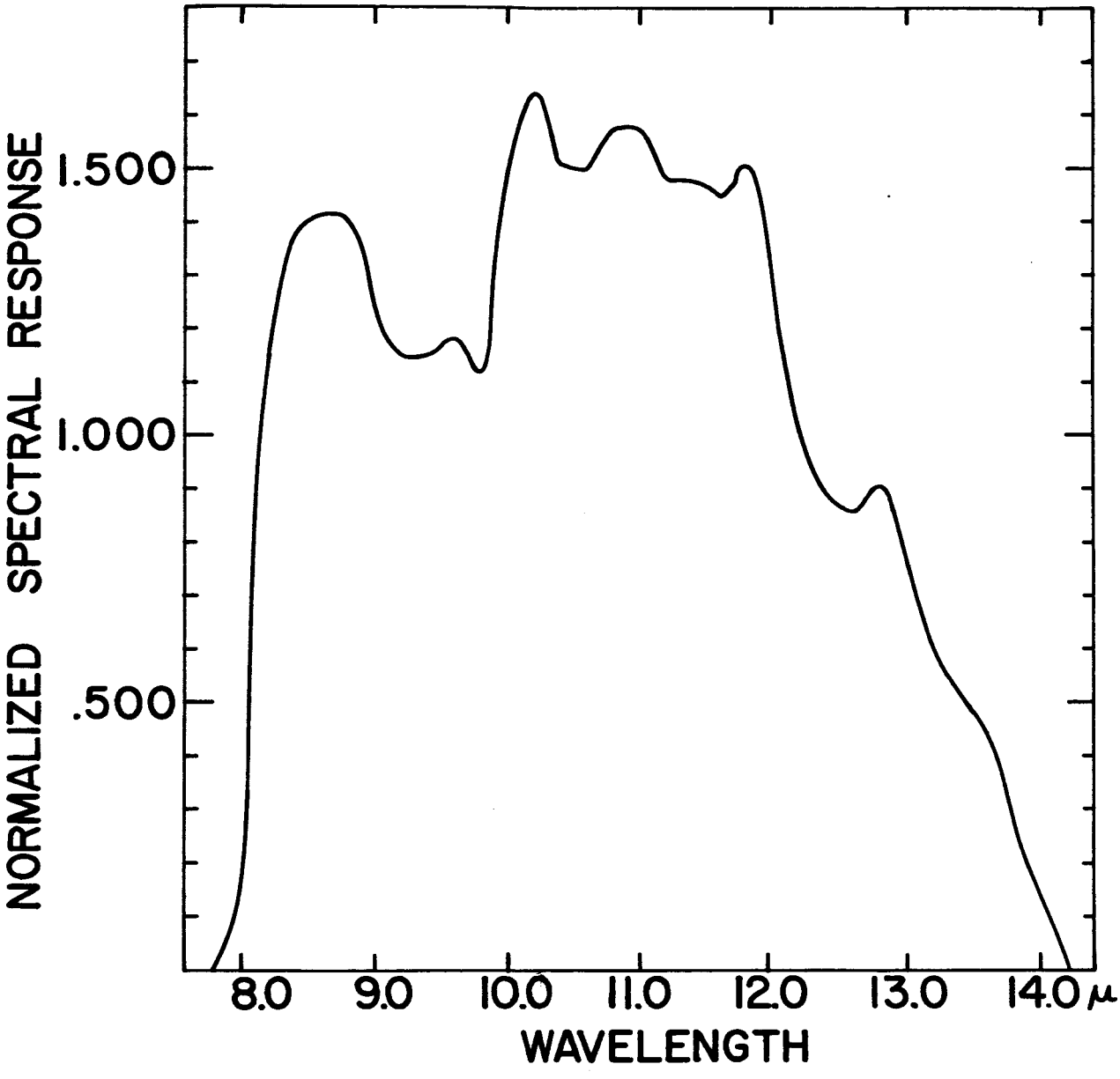

FIGURE 1

Spectral response of the photometer normalized to mean value of unity. Original measurements were obtained through the courtesy of the Naval Ordnance Research Laboratories, Corona, California.

In front of the cold cavity is a focal plane aperture. The f/15 beam of radiation from the primary mirror is made to form a real image on this aperture by means of the dual-beam photometer illustrated in Figure 2. A 0.6 mm aperture was used for the lunar observations corresponding to 17 seconds of arc at the focal length used. Thus the photometer presents the Fabry lens with the f/15 radiation emanating from a 17 second of arc circular area in the focal plane. The image placed on the focal plane diaphragm is, in effect, switched by the photometer at 180 cps from that of a small portion of the lunar surface to that of an equal angular area of sky beside the moon and back again. The switching is closely "square-wave" and does not involve any image motion . The cell thus "sees" the primary mirror fluctuate in brightness at 180 cps. The alternation in total incident 8-14 micron radiation between the two halves of the switching cycle leads to a small phased-locked square-wave voltage fluctuation which is amplified, synchronously rectified and recorded on a strip chart recorder. The spectral response of the system is known and the photoconductive cell is not known to depart from a constant monochromatic responsivity within the intensity range of the present observations. Hence, the deflection on the strip chart recorder can be directly related to the difference in incident radiation between the two halves of the switching cycle, i.e., to the intensity of the lunar radiation in the 8-14 micron interval, reduced by atmospheric and telescope transmission losses.

The photometer was used at the f/15 "bent" cassegrain focus of a portable 20 inch telescope designed and fabricated especially for lunar infrared observation. The f/2 primary was made available by the Mount Wilson and Palomar Observatories. All mirrors were gold-surfaced because

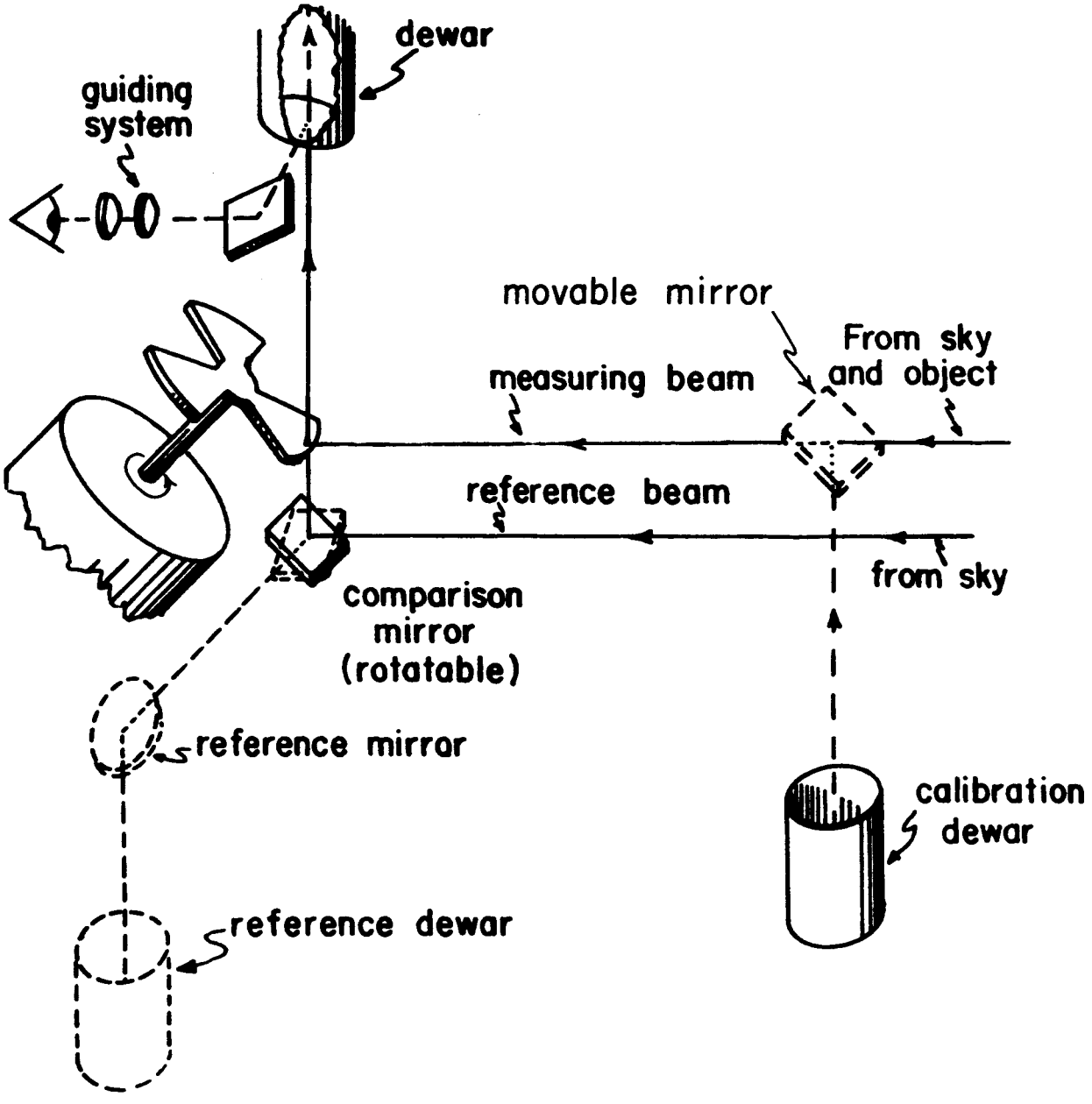

FIGURE 2

Schematic diagram of optical paths through double-beam photometer. Calibration mode indicated by dashed lines.

published data (Allen, 1955; Harris and Fowler, 1961) indicate that gold-surfaced mirrors should be superior to aluminum-surfaced ones in the 8-14 micron region. The telescope was located in a small observatory utilizing a prefabricated dome at an elevation of 12,800' on White Mountain, California. White Mountain is east of Bishop, California, nearly at the Nevada line with $\lambda = 118^{\circ}$ W and $\phi = +37.5^{\circ}$. The University of California operates a high-altitude research station there making it convenient also for our operations. Lunar observations discussed in this paper were collected there during August and September of 1962.

b) Formal Relationships and Calibration Procedure

To develop the formal relationships, we shall begin with the deflection and proceed "backward", as in a).

$$D = GV_o \tag{1}$$

where: D = Deflection on strip chart recorder in volts.

G = Electronic gain through a linear electronic system.

V_o = Average AC output voltage of cell during integration time of electronics and recorder, between 0.1 sec and 1.0 sec.

Since the modulation (chopping) period, 1/180 sec., is very small compared to the electronic integration time, 1/10 to 1 sec., but very long compared to the intrinsic time constant of the cell, 10^{-6} sec., and, further, since the modulation is closely "square wave",

$$V_o = \Delta V_{ab} + V_{cn} \tag{2}$$

where: ΔV_{ab} = AC output voltage of cell due to modulated incident radiation averaged over the integration period.

V_{cn} = Average AC output voltage during integration time from cell due to other sources, i.e., Johnson noise, microphonic effects, current noise, etc. For the applications of this paper, $V_{cn} \ll \Delta V_{ab}$ and will not be included further.

Therefore: $$V_o = \Delta V_{ab} \tag{2a}$$

The monochromatic responsivity R_λ of photoconductive cells is a function not only of cell temperature and intrinsic cell properties, but also of the "background" flux (Smith, Jones, and Chasmar, 1957; Bratt, et al., 1961). No non-linearity has been detected over the range of background fluxes encountered in either the

observational or calibration modes of the present investigation*. Accordingly, the relationship between incident radiation and output voltage is:

$$\Delta V_{ab} = \frac{D}{G} = r \int_{8\mu}^{14\mu} S_\lambda \left[W_\lambda (A) - W_\lambda (B) \right] d\lambda \qquad (3)$$

where: r = 8-14 μ responsivity (a constant with units of volts/watt).

S_λ = Normalized spectral response (See Figure 1).

$W_\lambda(A), W_\lambda(B)$ = Incident flux during two parts of chopping cycle.

Expansion of the incident flux terms gives,

$$D = G\, r\, \bar{\rho}\, A \Omega \int_{8\mu}^{14\mu} S_\lambda \left[B_\lambda (T_b)\, E_\lambda (\mathrm{Sec}\ Z) \right] d\lambda + \left[Q + q(t) \right] \qquad (4)$$

where: $\bar{\rho}$ = Transmission coefficient of telescope (but not photometer). Included in this coefficient is an obscuration factor for the secondary mirror.

A = Area of focal plane aperature.

Ω = Area of primary mirror divided by square of effective focal length.

$B_\lambda(T_b)$ = Spectral brightness corresponding to lunar brightness temperature in the 8-14 μ region, T_b.

$E_\lambda(\mathrm{Sec}\ Z)$ = Atmospheric spectral transmission corresponding to zenith distance of observation.

$[Q+q(t)]$ = Imbalance displayed on recorder arising from instantaneous differences in sky and telescope emissions as viewed through the two beams. Q is the mean value (during a particular observation time) and q(t) is the random (but not "white noise") time fluctuation. For the observations in question, $Q \gg q(t)$, and is always measured by looking at the sky only with both beams.

*It should be noted, however, that direct simulation in the laboratory of the kinds of signal and background fluxes encountered in lunar observations through the telescope is beyond our present capability. Consequently we are, in effect, extrapolating determinations of responsivity rather than interpolating them.

Finally, if S_λ is known and an atmospheric transmission model assumed, one can define,

$$b\ (T_b,\ \text{Sec}\ Z) = \int_{8\,\mu}^{14\,\mu} S_\lambda\ \left[B_\lambda(T_b)\ E_\lambda(\text{Sec}\ Z)\right]\ d\lambda \qquad (5)$$

and,

$$N\ (T_b,\ \text{Sec}\ Z) = \frac{b\ (T_b\ ,\ \text{Sec}\ Z)}{b\ (273^\circ K,\ 0)} \qquad (6)$$

The function N (T_b, Sec Z) for the S_λ of Figure 1 and the atmospheric transmission model used in the reduction of the present observations (Figure 4) ~~are~~ is shown in Figure 3. Accordingly the relationship for the net deflection (D-Q), assuming q(t) to be small, is:

$$D\text{-}Q = G\ r\ \bar{\rho}\ A\ell\ N\ (T_b,\ \text{Sec}\ Z)\ \ b\ (273^\circ K,\ 0) \qquad (7)$$

The calibration mode of the photometer provides a means of viewing a water-ice black-body cavity and a liquid nitrogen black-body cavity through the same solid angle as is subtended by the primary mirror. Thus the deflection (D-Q) corresponding to 273°K can be observed directly. Accordingly,

$$(D\text{-}Q)_{273^\circ K} = G\ r\ A\ell\ b\ (273^\circ K) \qquad (8)$$

Substituting, one gets,

$$N\ (T_b,\ \text{Sec}\ Z) = \frac{1}{\bar{\rho}}\ \frac{D\text{-}Q}{(D\text{-}Q)_{273^\circ K}} \qquad (9)$$

Thus equation (9) gives N (T_b, Sec Z) in terms of observable or known quantities, and Figure 3, the calibration curve, relates the N (T_b, Sec Z) to the 8 - 14μ lunar brightness temperature.

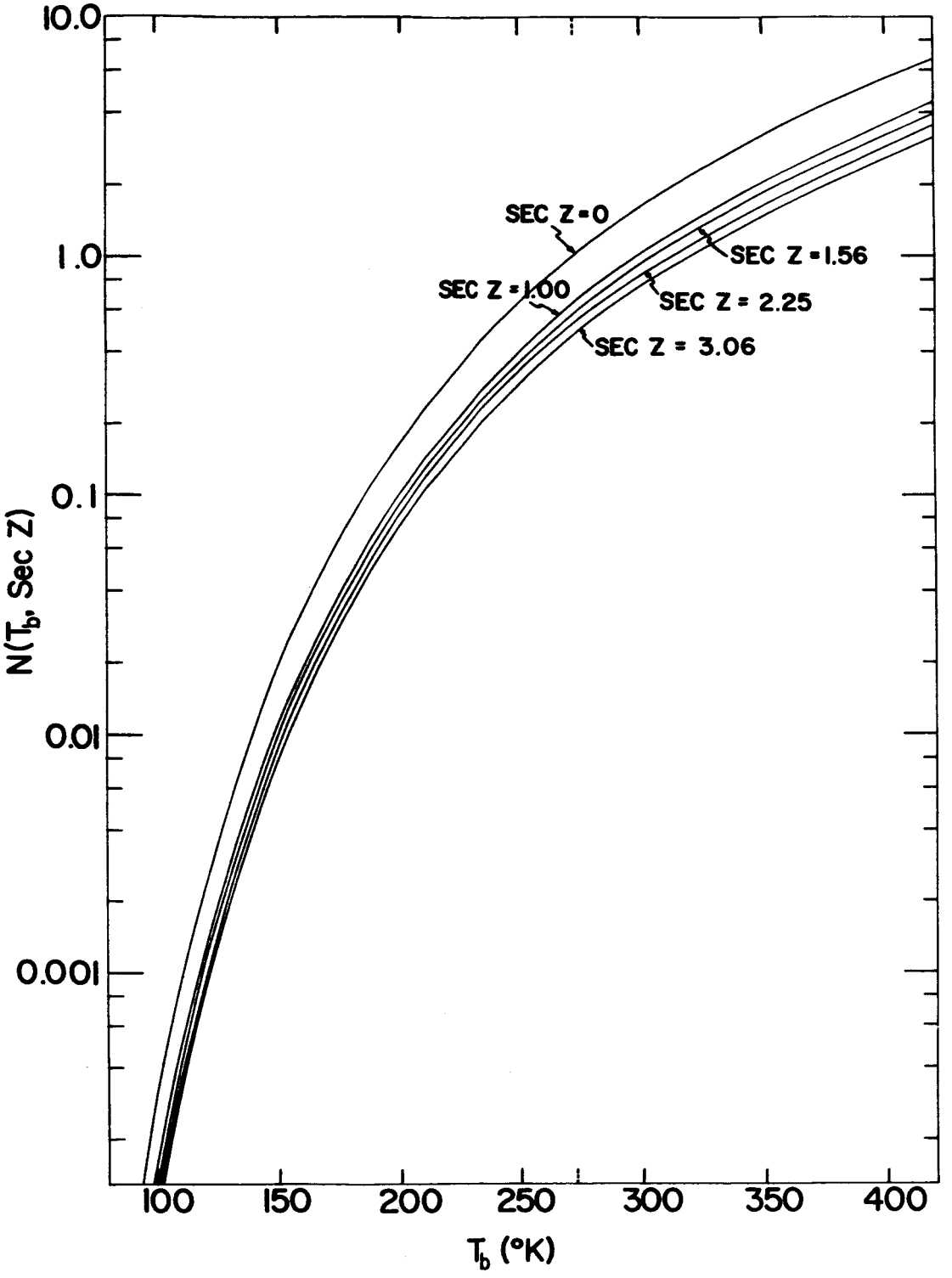

FIGURE 3

Calculated response of photometer to radiation from extended objects outside atmosphere. Atmospheric transmission losses for various paths lengths are also included. The response has been normalized to that for 273°K and no atmospheric transmission losses.

c) Transmission Losses and Estimates of Accuracy

The spectral transmission of the atmosphere in the 8-14 micron region has been the subject of both theoretical and observational investigation for many years. However, neither the dependence of extinction on zenith distance, nor the range of variability in extinction that can be expected are firmly established at the present time. Furthermore, the reflectivity of our gold-surfaced mirrors appears to be appreciably lower than the 99% suggested by published data (Harris and Fowler, 1961). It would be desirable to handle such transmission losses by use of nightly determination of extinction and reflection losses from observations of "standard" planetary or stellar objects. Unfortunately, only one possible "standard" object (Jupiter) was available for use with our 20" telescope at White Mountain, and there is no independent knowledge of the actual 8-14 micron brightness temperature of Jupiter. Accordingly, a modified form of the extinction model of Sinton and Strong (1960, a,b) was used. Despite the limitation of being able to observe only one "standard" celestial object, the repeated observations of Jupiter over a moderate range of secant zenith distance provide a measure of the nightly variability of combined extinction and calibration errors, as well as a means of detecting any gross systematic error in extinction.

The Sinton and Strong extinction model utilizes a square-root dependence on the secant zenith distance. The spectral distribution of atmospheric transmission measured at Mount Palomar (elevation 5750') for a secant zenith distance of 2.25 is shown as the lower curve in

Figure 4. In order to approximately interpolate their results to the White Mountain site (elevation 12,800') we have applied a simplified* transformation:

$$\ln\left(\frac{A_p(\lambda)}{A_w(\lambda)}\right) = \frac{P_p}{P_w}$$

where: $A_p(\lambda)$, $A_w(\lambda)$ = Coefficients of atmosphere transmission for Palomar and White Mountain, respectively.

P_p, P_w = Ambient pressure at Palomar and White Mountain, respectively.

The resulting transmission curve is shown as the upper curve in Figure 4. Extinction coefficients for values of other secant zenith distances have been obtained analogously and the results incorporated in the N (T_b, Sec Z) curve shown in Figure 3.

The random errors introduced by using an assumed extinction model rather than an observed one can be roughly estimated from the nightly variations in the apparent brightness temperature of Jupiter. This observed variance includes, in addition, a measurable variation in responsivity of the cell. Also, Jupiter shows strong limb-darkening (in subsequent 200 inch observations with the same photometer and cell). Since at White Mountain the focal plane diaphragm for lunar observations was about 1/3 the size of the planetary image, there was considerable variance in the deflection arising from inexact centering of the Jupiter image on the diaphragm, a problem not characteristic of the lunar observations. Nevertheless, the observations of Jupiter for 12 different nights yield a

*This transformation ignores the differential effects of pressure broadening, the existence of which is implied by the square-root dependence of the law.

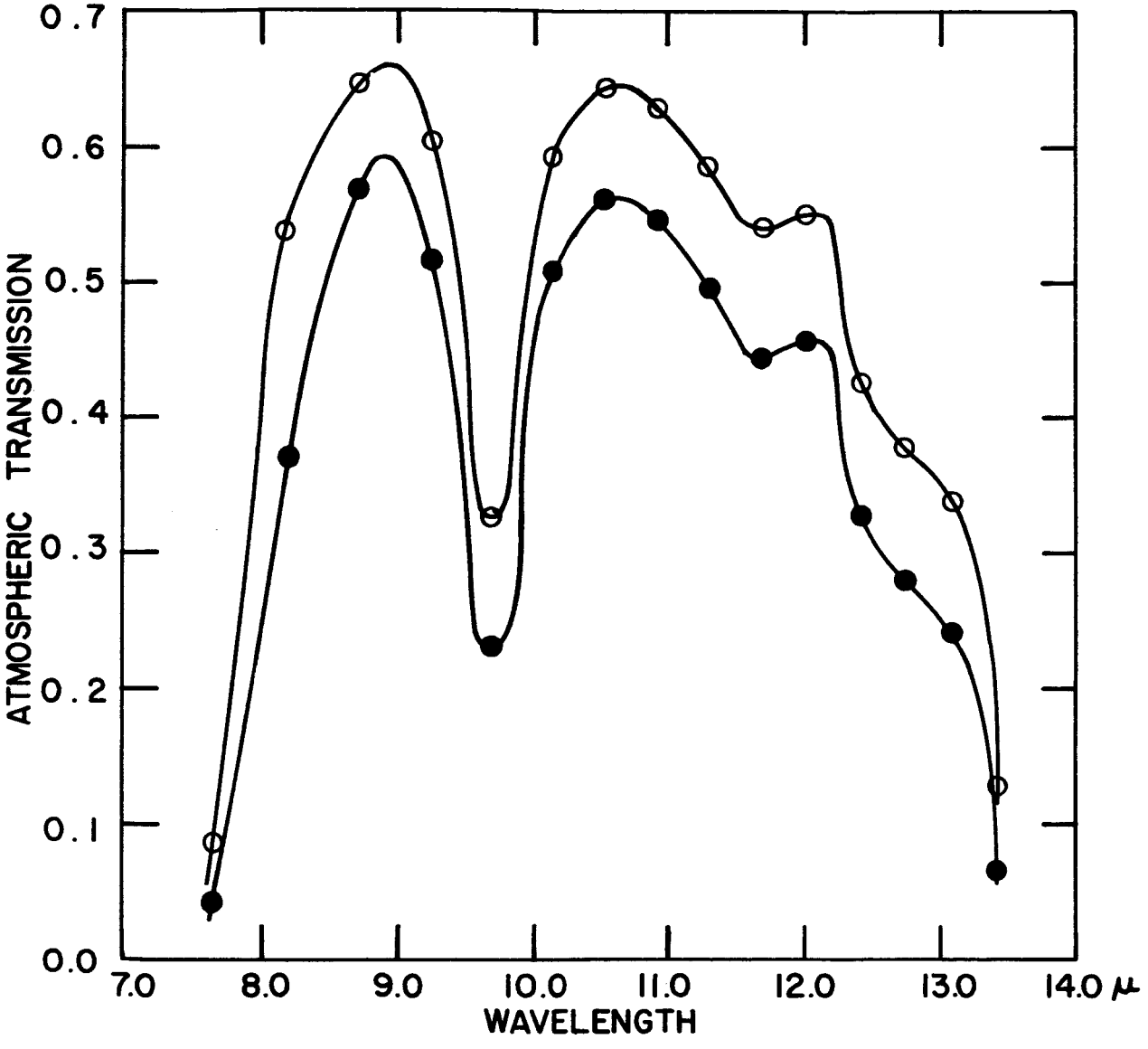

FIGURE 4

Atmospheric spectral transmission for 2.25 air masses. The open circles is that reported by Sinton and Strong (1960 a,b) for Mount Palomar, and the filled circles is that assumed in the present paper for White Mountain.

mean value of 128°K with a standard deviation of ± 2.3°K when reduced in the same manner as were the lunar measurements. Accordingly, we take ± 3°K at 128°K to be a reasonable upper limit for the nightly random error in the lunar observations. In addition, there are at least two obvious sources of systematic error. The first is the extrapolation to secant zenith distance = 0 which is quite sensitive to the functional form of the zenith distance dependence. The second is the real transmission loss within the telescope. In the reduced Jupiter data there is a slight trend for the apparent brightness temperature to increase with increasing secant zenith distance indicating that the deflections may have been overcorrected for supposed extinction losses. This trend is eliminated, or possibly even slightly reversed, if no extinction correction at all is used. The mean value of the brightness temperature is reduced 7°K by this procedure. It seems possible that our reduced lunar values may be systematically too high up to perhaps 5°K, for a temperature of 128°K, because of extinction overcorrection. On the other hand, we have assumed the transmission coefficient of the telescope (including the secondary mirror) to be unity. Actually it could be no larger than about 0.94* even if the mirrors had the 99% reflectivity indicated in the literature. Rough measurements in the laboratory of gold-surfaced mirrors similar to those on the telescope suggest a reflectivity of about 0.93 leading to an estimate of about 0.8 for ρ. Such an instrumental transmission loss, not allowed for in the data reduction, leads to brightness temperatures systematically too low by 2.5°K at 128°K. The two primary sources of possible systematic error thus have a compensating effect on

*The obscuration due to the secondary mirror is about 4%.

the reduction procedure used for the lunar observations discussed in this paper. Accordingly $\pm 5^{\circ}K$ is adopted as the likely upper limit of systematic errors and $\pm 3^{\circ}K$ as the likely upper limit of random night-to-night errors in the lunar observations presented here.

TABLE I

ESTIMATED ERRORS IN LUNAR BRIGHTNESS TEMPERATURE

(For $128^{\circ}K$ Lunar Observation)	
Random (night-to-night)	$\pm 3^{\circ}K$ (25% in flux)
Systematic	$\pm 5^{\circ}K$ (40% in flux)

Finally, we can consider the differential accuracy of a given scan and the minimum detectable temperature of the entire system. Examination of the tracings of actual strip chart records shown in Figures 6 and 7 shows both a "white" noise originating within the cell itself and also a distinct pattern of fluctuations in the 10 - 100 sec period range.

These "low frequency" fluctuations arise from non-stationary emission originating in the telescope and in the atmosphere as viewed by the double-beam photometer. Scan VIII is included to illustrate a night when this low frequency noise was particularly strong. In general, the low frequency noise was the limiting noise for the determination of temperatures on the lunar scans and resulted in a minimum detectable brightness temperature of about 105°K for a small area on the moon. Thus the differential accuracy in temperature measurement of a given scan is generally limited to a deflection reading corresponding to 105°K. In terms of signal-to-noise ratio the differential accuracy (or "reading" accuracy) in temperature is illustrated by the following table, derived from Figure 3:

TABLE 2

DIFFERENTIAL ACCURACY OF SCANS

Lunar brightness temperature (°K)	Approximate signal-to-noise ratio
105	1:1
115	2.5:1
125	6.5:1
135	12.5:1
145	24:1
155	43:1
165	69:1

There is no electronic integration in the above data; the effective low pass filter of the system is the recorder itself, with time constant of about 1/4 sec. It should also be noted that the vertical scale is not the same in each of the scans.

III THE OBSERVATIONS

a) Introduction

The observations discussed in this paper were obtained on the nights of 21-22, 23-24, and 24-25 August, and 22-23 September, 1962. Tracings of some of the original strip chart records are shown in Figure 6. The scan tracks of all the observations used are plotted in Figure 5. Right ascension scans were begun just sunward of the evening terminator and carried across most, or all, of the shadowed lunar surface and then reversed in direction until the terminator was again crossed. The reversal point was far enough from the terminator that the lunar temperature was usually below the system noise level and, hence, the reversal point could be taken to be a measurement of "sky only" to provide a deflection zero reading. The reference beam of our double-beam system was always either on the sky or on a part of the dark moon far enough from the terminator to have no detectable emission. In addition, the telescope was moved off the moon before and after most of the scans to provide additional zero deflection readings. The non-coincidence of forward and reverse scans is due to the motion of the moon in declination. We were unable, therefore, to repeat the exact geographic coverage of each scan, which is one reason why the anomalous features illustrated in Figure 6 do not reproduce exactly between the left and right sides of the figure. The linear spacial resolution of the measurement, allowing for diffraction and seeing, is 26 seconds of arc, corresponding to about 50 kms. at the sub-earth point of the lunar surface.

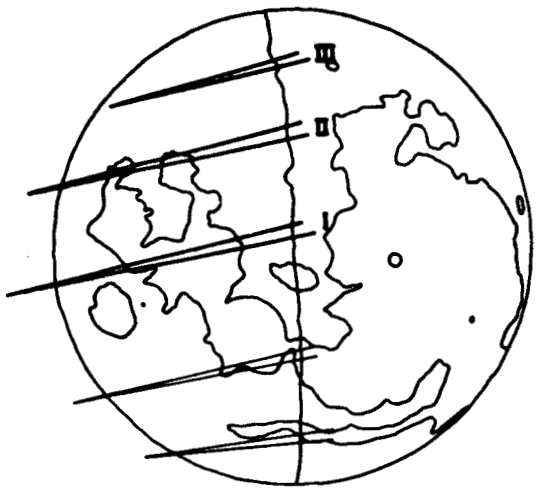

AUG 21-22 1962
22.0 DAYS
11h U.T.

AUG 23-24 1962
24.0 DAYS
13h U.T.

AUG 24-25 1962
25.0 DAYS
13h U.T.

SEPT 22-23 1962
23.4 DAYS
12h U.T.

FIGURE 5

Locations of lunar right ascension scans discussed in this paper with date and time of observations and age of moon. The systematic skewing of the scan lines between nights is an effect of plotting onto a single lunar projection corresponding to a somewhat different libration than each of the individual nights. Scans identified by a roman numeral are reproduced in Figures 6.

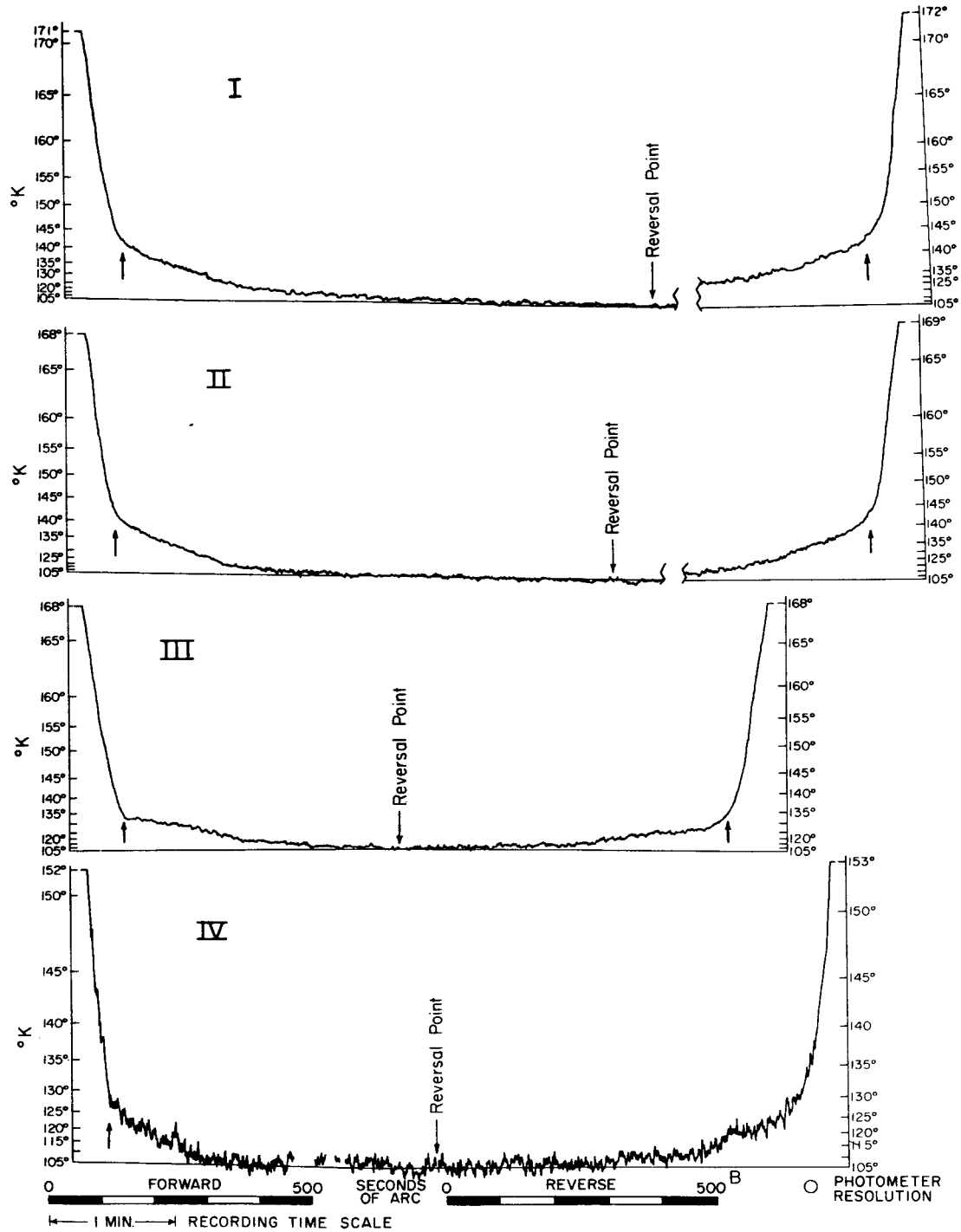

FIGURE 6

Tracings of strip chart recordings of voltage deflection vs. time for scans indexed in Figure 5. Reduced brightness temperatures in °K are also shown in the vertical scale. The time base of the recordings is shown along with a scale illustrating the angular displacement in seconds of arc. The terminator, with a brightness temperature of 200°K or greater is off scale on the tracings, but is located twice in each scan between the abscissa points at the very beginning and ending of each scan, where the recorder pen was "pegged", and the points where the deflection was a maximum and on-scale.

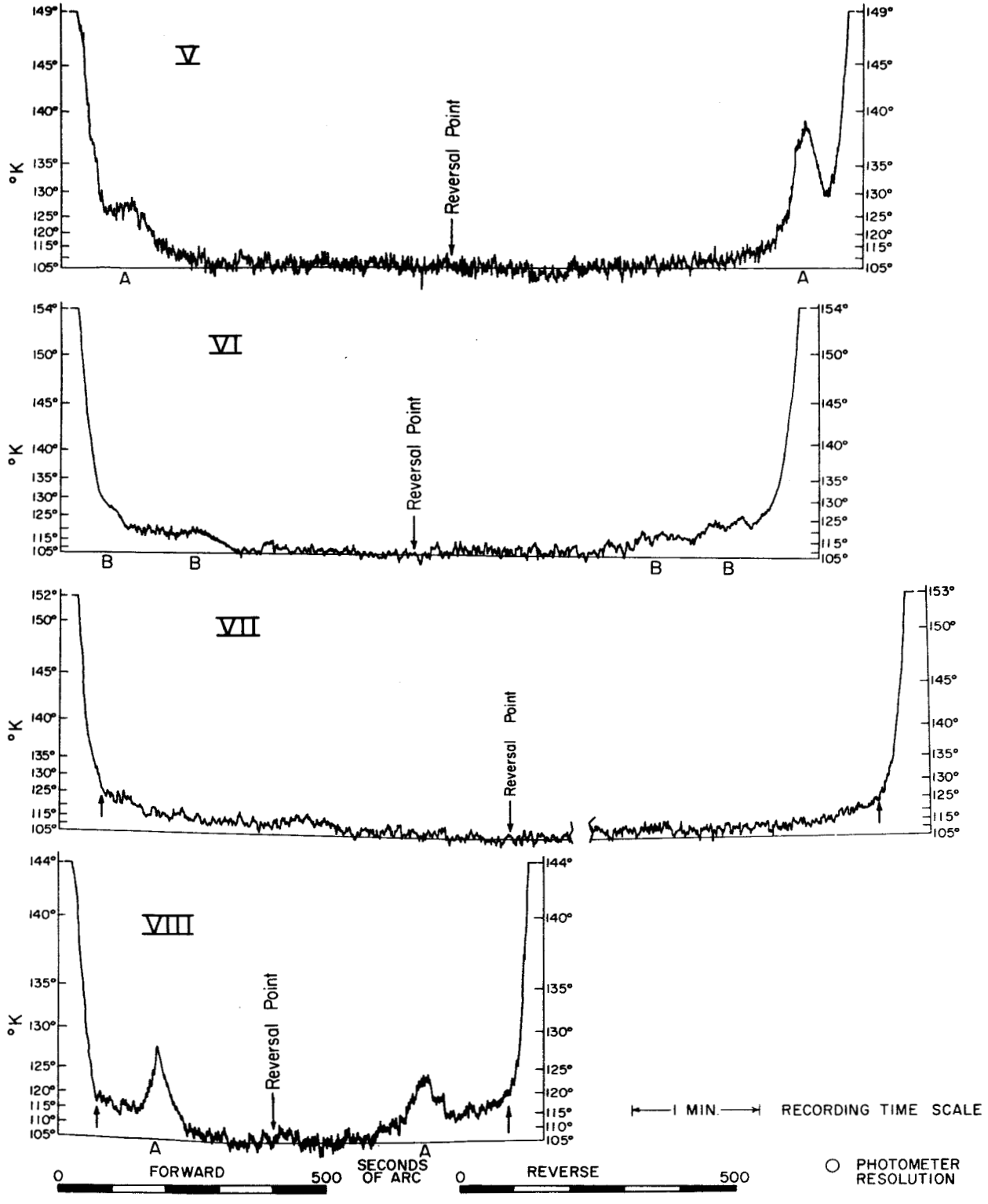

FIGURE 6 (continued)

Scans I, II and VII have been broken in order to facilitate presentation here. The arrow denotes a characteristic abrupt change in slope. The letters A and B refer respectively to definite and to probable or possible anomalies.

Accurate, continuous determination of position of the focal plane aperture with respect to the image of the unilluminated lunar surface is a formidable problem. The positional information required to produce Figure 5 was obtained by taking 35 mm photographs at the beginning, reversal and ending points of each scan through a small finder telescope. A reticle in the optical train of the finder provided a crosshair pattern superposed on the lunar image. These crosshairs, which could also be observed visually through a separate eyepiece, were aligned to correspond with the photometer aperture position by setting on a small prominant illuminated lunar crater. Additional photographs were sometimes taken at the time of crossing a prominant temperature anomaly and served to better pinpoint related positions. The positional errors resulting from the difficulty in reading positions accurately on such low resolution photographs are significant, but probably do not correspond to more than 2-3 times the geographic resolution. In some instances, however, the setting of the finder with respect to the photometer was disturbed and a systematic shift introduced. Since additional check photographic positions were usually acquired during the run such systematic errors could sometimes be corrected. However, systematic positional errors of perhaps 5 times the resolution may still persist.

b) Variation in Brightness Temperature with Selenographic Longitude

Scans I through VIII have been selected to illustrate not only typical scans, but also local anomalies, the effects of poor observing conditions, and the effects of variations in latitude and phase angle. The general form of the variation of brightness temperature with longitude persists, however. It is characterized by three features: (1) A very steep gradient (perhaps even steeper than indicated because of the finite photometer resolution) in the first six degrees (12 hours) or so into the lunar nighttime, (2) In most cases a rather abrupt change, in the temperature range 120°K - 145° K, to a more moderate slope, and (3) Continued decrease in brightness temperature until the system noise level of 105°K (referred to outside the atmosphere) is reached.

In Figure 8 the forward and reverse halves of scan I have been averaged and replotted in a linear diagram of brightness temperature vs. selenographic longitude. The form of the curve in Figure 8 seems to be characteristic of brightness temperature vs. longitude elsewhere on the lunar surface except that the temperature at which the gradient becomes more moderate is lower at higher latitudes and at later lunar ages, and the temperature seems to fall below the 105°K limit after a somewhat shorter duration of lunar nighttime in these cases. There also seems to be a tendency for the change in gradient to be somewhat more abrupt at higher latitudes (i.e., scans III and VII).

c) Local Anomalies in Brightness Temperature

As is illustrated in scans IV, V, VI, and VIII, anomalously "hot" regions occur. The term anomalous is used here in a geophysical sense, i.e., denoting a local departure from a regional pattern of variation of a physical quantity. Class "A" anomalies, considered to be definite evidence of a local variation in surface thermal properties, are those in which a clear reversal of slope occurred on both the forward and reverse portions of the scan. Class "B" anomalies, regarded either as probable or possible evidences of anomalous thermal properties, include those in which only a flattening was observed instead of a clear reversal or in which the feature did not reproduce satisfactorily on both the forward and reverse parts of the scan.

The upper part of Figure 7 shows the locations of the anomalies encountered on the scans of Figure 5. The lower part of the figure is an index map. It can be seen that there are groupings of definite anomalies around Tycho and Copernicus and also class B anomalies in two otherwise undistinguished areas along mare borders. The anomalies detected on individual scans, at least in the case of Tycho and Copernicus, are definitely part of an association of anomalous thermal properties of larger geographic size than either of the rayed craters in question. Also the anomalies intersected on a single scan, i.e., IV, V, VI, or VIII, are generally larger than the photometer resolution, and, indeed exhibit considerable structure. Thus, it appears that at least Tycho and

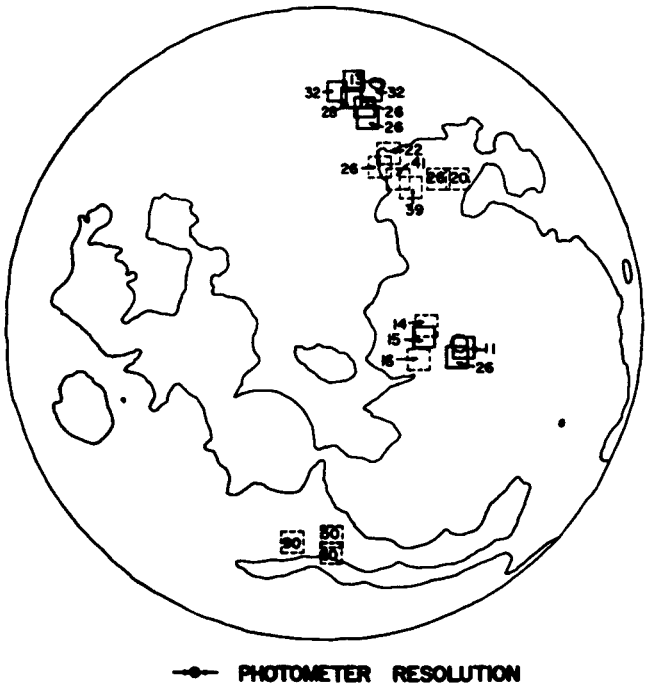

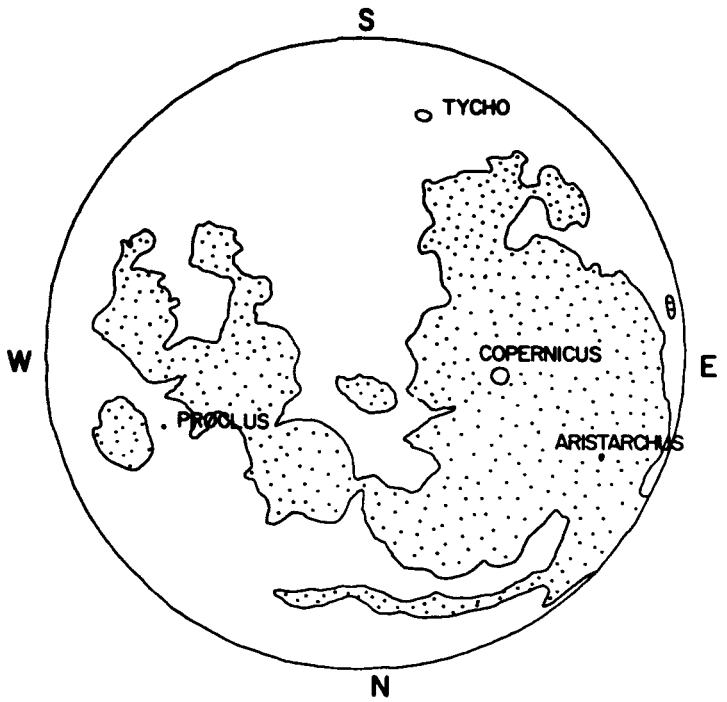

FIGURE 7

Locations of anomalies in 8 - 14 μ brightness temperature detected in scans shown in Figure 5, along with lunar index map. Solid line squares are definite anomalies, examples of which are indicated by the symbol A in Figure 6. Dashed line squares are probable or possible anomalies, example of which are indicated by the symbol B in Figure 6. The number inside the square is the approximate number of hours since passage of the terminator.

Copernicus are each associated with a complex of anomalies, not just a single anomaly identical with the crater itself. It should be noted that since there is evidence of detailed structure below the photometer resolution as well as overall size larger than that resolution, the apparent peak temperature encountered, for example 138°K in scan V, is only a lower limit for what the real brightness temperatures of some, perhaps significant, portion of what that 50 km circular area may include.

A thorough search was made of the Tycho area near first quarter, i.e., 10-12 days into the lunar nighttime, without any lunar radiation detected.

The two anomalous regions in the mare border area both have a few small rayed craters that may be associated with the anomalies. It may well be that thermal anomalies are generally characteristic of bright rayed craters.

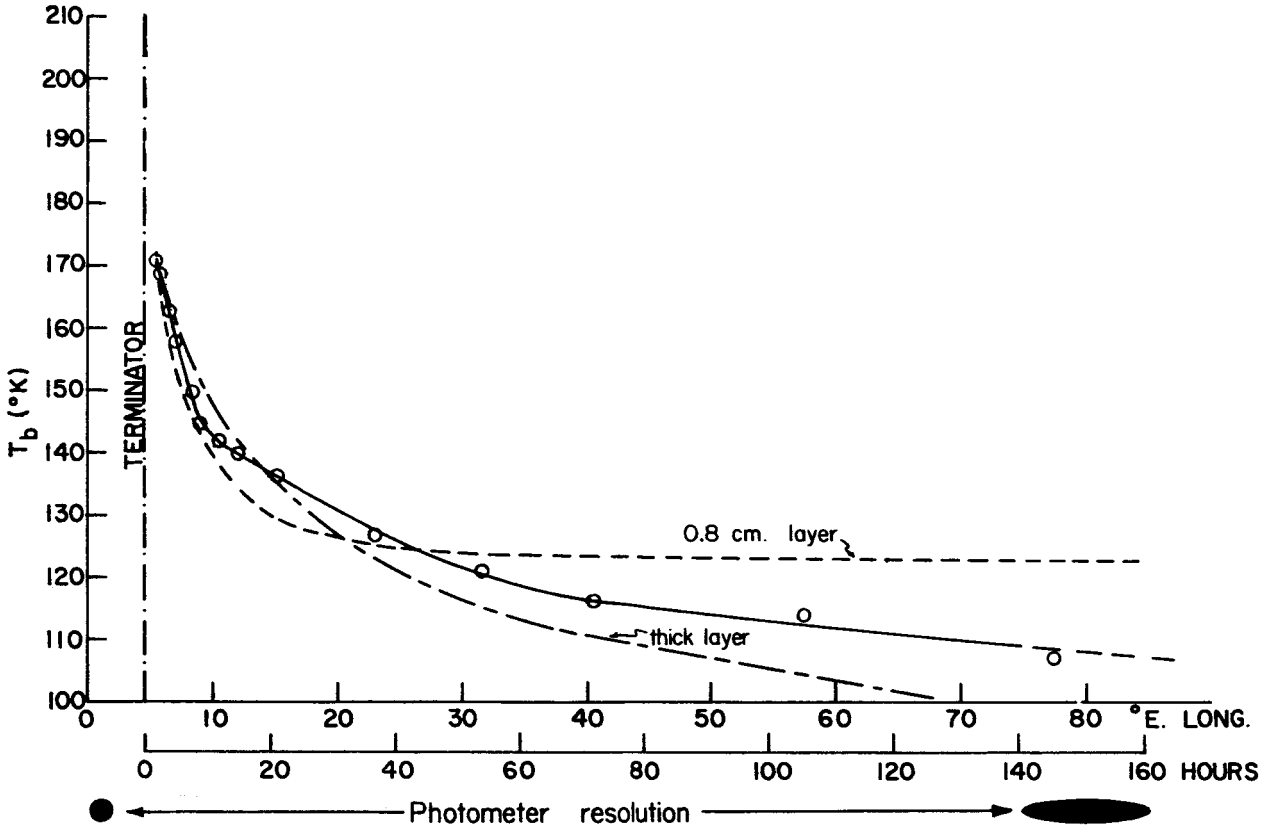

FIGURE 8

8-14 μ brightness temperature vs. lunar longitude (and time since passage of terminator) reduced from deflections of scan I, August 21-22, 1962. Forward and reverse halves of the deflections on that scan were averaged to eliminate effects of any linear base line drift. Circles represent individually reduced data points. Also shown in dashed lines are theoretical lunar surface temperature vs. time curves enlarged from Jaeger (1953) adjusted to pass through the 170°K point of the observed curve. The lower dashed curve is that derived for a single "thick" insulating layer of $(k\rho c)^{-\frac{1}{2}} = 1000$. The upper dashed curve is for the case of an 0.9 cm layer of such material on top of a more conductive ($[k\rho c]^{1/2} = 20$) layer. The thermal properties were assumed to be independent of temperature in Jaeger's analysis.

IV DISCUSSION

a) Introduction

In order to interpret the observations just discussed, the relationship of observed brightness temperature to actual lunar surface temperature must be examined. In reality, there is no a priori reason the 8-14 micron radiation from the Moon need resemble exactly that of a blackbody in spectral distribution, absolute intensity or directional variation. Several lines of evidence permit an estimate of lunar departures from blackbody conditions. It will be seen that the Moon very probably does resemble a blackbody sufficiently to permit the present brightness temperature observations to be considered as measurements of lunar surface temperature within the observational accuracy limitations already discussed, except in the extreme limb regions of the Moon.

The overall spectral distribution of thermal radiation emanating from the Moon shows the effects both of an increase in transparency with wavelength and of a time-dependent vertical temperature gradient. Whereas the time variation of the infrared brightness temperature is totally dominated by the diurnal (lunar) variation in insolation, 21 cm observations (Sinton, 1962) show no detectable lunar phase effect indicating that the optical depth characteristic of such wavelengths corresponds to a physical depth well below the region of diurnal temperature variation. Variations in transparency of the surface materials within the 8-14 micron region itself might be expected if the particles at the very surface were extremely fine, (around 5 microns or smaller) and, if these grains are fragments of crystalline or cryptocrystalline silicate minerals. Silicate minerals,

which make up virtually the entire crust of the earth, are characterized by strong absorption bands in the 8-14 micron region corresponding to resonances of the different forms of silicon-oxygen bonding within the crystal lattice (Launer, 1952). In the conventional measurement of these absorption bands in the laboratory, the mineral is powdered to 5 microns or less in grain size and deposited as a very thin layer on a sodium chloride window in an infrared spectrometer. The temperature gradient within the surface layers of the Moon appears to be so steep at times that the brightness temperature in the 8-9 micron region may be significantly different than that in the 9-10 micron region where a strong absorption band commonly is present. Even assuming favorable conditions, however, a departure from black-body emission arising from this mechanism cannot be expected to produce effects comparable to the estimated night-to-night and systematic errors discussed in section II. On the other hand, the possibility cannot be entirely rejected that weak temperature anomalies, like some of those of the "B" category of section III, might arise from a local concentration of a mineral suite with markedly different absorption characteristics than those of the surrounding surface materials. It does seem prudent at this stage of our knowledge - and ignorance - of the moon to leave open the interesting possibility of such minor departures from black-body (and even gray-body) emission of lunar surface materials.

Another characteristic property of silicates leading to a possible departure from black-body emission was of concern to Pettit and Nicholson (1930). This is the property of enhanced reflectivity of slabs, and to a lesser extent, of coarse aggregates of quartz and other silicates. This anomalous reflectivity arises from a disturbance of the index of refraction

generated by the same resonances which cause the absorption bands, but at slightly shorter wavelengths. The residual ray reflection exhibited by smooth surfaces of quartz and other crystalline substances was the basis of the first infrared filters, the Rubens plates, and has continued in use through the recent work of Sinton and Strong. Pettit and Nicholson (1930) tested the assumption that the Moon's surface exhibited a reduced emissivity (integrated over 8-14 microns) as a consequence of the residual ray phenomena. They showed that the emissivity of the lunar surface must be nearly unity, within the accuracy of their work, inorder that the brightness temperature of the subsolar point / not exceed that theoretically possible on the basis of solar heating and reradiation. They also pointed out that this didn't make silicates any less likely candidates for major constituents of the lunar surface, but merely required that the material be in powdered form, a result already required by the eclipse cooling data. Valuable new data have been obtained recently by Lyons (1963) pertaining to departures from blackbody emission by silicate aggregates. Sinton (1960) found it so difficult to reconcile the observed and expected brightness temperatures he even proposed occasionally enhanced solar radiation inorder to rectify the apparent discrepancy. It seems clear that the Moon is a black-body emitter to a first approximation in both spectral distribution and absolute intensity, but may have small - and extremely important - departures which can be investigated with more sensitive equipment.

The non-Lambert character of the lunar infrared radiation was found by Pettit (1935), in time-sequence observations of the specific intensity at the subsolar point. This effect may be primarily a result of macroscopic roughness and related shadowing, although it should be noted in

passing that any minor departures from black-body emission arising from the finite optical thickness of a lunar dust layer must also be accompanied by departures from Lambert emission.

b) Geophysical Significance of the Longitudinal Variation of Surface Temperature

The variation of nighttime surface temperature with longitude on the Moon can be considered to be a measure of the time variation of temperature at a single point in the absence of large scale geographic variations in thermal properties. Indeed, the initial temperature differences arising from variations in albedo are damped out so quickly that no effect is apparent on the scans as the contact between mare and upland areas is crossed. Accordingly, the two halves of scan I were averaged (to eliminate the effects of any linear error in base line) and plotted in Figure 8 as a function of selenographic longitude and also as a function of time since passage of the terminator. Figure 8 thus represents the portion of the cooling curve of an "average" equatorial area on the Moon for the first 160 hours or so of the lunar nighttime. The daytime portion of the cooling curve has been measured previously (Geoffrion, Korner, and Sinton, 1960; Pettit and Nicholson, 1930), but the nighttime portion previously had to be estimated from the higher temperature eclipse cooling observations. The eclipse cooling observations are only influenced by the thermal properties of the outermost few millimeters of the surface at the most and tell us little more than that thin skin is an exceedingly good thermal insulator. The present observations extend well into the lunar nighttime and provide the first direct investigation of the thermal properties of the Moon in the depth range of a few millimeters to a few centimeters. Microwave observations have been made at wavelengths as short as 1.5 mm (Sinton, 1955), but these observations probably still see "through" the layers presently being discussed. In

particular, the nighttime cooling curve can provide direct evidence of vertical and horizontal inhomogenities. The problem has been investigated theoretically (see discussion in and references at end of Sinton, 1962); we find the analysis of Jaeger (1953) to be the most useful for purposes of qualitative comparison of our observations with simple models. Jaeger computed both the lunation cooling curves and eclipse cooling curves for a thick layer of material with various values of $(k\rho c)^{-\frac{1}{2}}$ where k is the thermal conductivity, ρ the density and c the specific heat. He found that a value of $(k\rho c)^{-\frac{1}{2}}$ of about 1000 in calories and cgs units best satisfied the eclipse cooling observations of Pettit and Nicholson (1930). This corresponds to a value of $k\rho c$ about 2500 times smaller than that of consolidated rock and is consistent with the concept of a porous powder consituting the very outer skin of the Moon. He also considered the case where this skin is less than a centimeter thick and is underlain by a thick layer of more conductive material with thermal properties similar to consolidated rock. Layers substantially thicker than a few centimeters degenerate into a single layer case. In all his calculations he considered the thermal conductivity to be constant within each layer, recognizing, however, that a temperature-dependent conductivity might actually be the case. Without specific information on such a dependence, more refined calculations provide little additional enlightment.

Two of Jaeger's curves have been enlarged from his publication, entailing some loss in accuracy, but without change in assumptions. They are reproduced in Figure 8 for comparison. Both have been arbitrarily shifted in time to pass through the 170°K point of the observed curve. It can be readily seen that the observed curve tends to resemble the two layer model in the abruptness of the change in slope around 140°K, but falls to an asymptotic lower temperature limit closer to the single layer case. However, it is clear that neither curve fits at all well. In fact, it may not be possible to explain

the observed curve with any kind of layering; no matter what assumptions are made, however, a homogeneous layer of porous dust of centimeters to meters thickness is clearly ruled out.

It may be that horizontal variations in conductivity arising from bare outcrop or boulders on the surface is an attractive alternative. Such a configuration could probably produce at least as good a fit as can the vertical variation model without exceeding the 10% or so limit to the areal extent of meter wavelength scattering material imposed by radar observations; (Evans, 1962). In any case, it can be concluded that conductive material must either be exposed at the surface or within a few centimeters of it over most of the Moon. In particular there appears to be no difference between mare and upland areas in this regard, a result of considerable importance to theories of dust on the Moon since it would now seem possible for there to be significant amounts of porous dust only if this is mixed uniformly with blocks of consolidated rocks i.e., resembling a breccia. Such a deposit might well characterize the lunar surface if an equilibruim existed there between rock consolidation processes and rock degradation processes (i.e. impact).

c) Geological Implications of Local Temperature Anomalies

Far more complete and accurately positioned infrared observations - and also specialized laboratory studies - will be required before a quantitative interpretation of the thermal properties of the local anomalies can be carried out. For the present one can only discuss their significance in a most qualitative way. Even so, these observations have strong implications regarding the nature of geologic processes operative on the lunar surface.

The local departures from the general pattern of longitude-dependent cooling are all positive, suggesting a pattern of local exposures of more conductive surface materials. Natural heat sources appear to be ruled out as a cause of the presently-observed local anomalies because of the enormous power requirements to maintain such large surface temperature differences over tens or hundreds of square kilometers. Also, the Tycho anomalies, at least, appear to disappear during the nighttime, as would be expected of diurnal heating and cooling. Near Tycho and Copernicus, these anomalous surface deposits appear to be distributed somewhat irregularly over an area considerably larger than the rayed crater itself. These same rayed craters display a lower daytime temperature - due to higher albedo - than do the surrounding areas (Shorthill and Saari, 1961); hence the anomalous nighttime temperature phenomenon does not reflect in any way differences in total absorbed daytime solar radiation. It is clear that a significant fraction of the surface within and about these two most prominent and very probably "recent" lunar impact craters is not covered with the same amount of the highly insulating dust which characterizes the great proportion of the lunar surface. It is likely, however, that at

least a very thin veneer of dust is still present; otherwise, corresponding anomalies in visible polarization (Dollfus, [redacted], 1962) and brightness versus phase observations (Wildey and Pohn 1963, in preparation; Van Diggelen, 1960) would also characterize these same craters. Hence, it seems likely that the conductive material is covered by only a thin layer, perhaps less than one millimeter in thickness of the extremely insulating dust. Nearly bare consolidated rock outcrop is thus suggested (including in this term compacted and cemented dust, or dust and impact debris, as well as crystalline rock) or possibly a dense distribution of large blocks. Also, secondary impact craters clustered about the primary craters should also provide considerable exposures of consolidated rock. A very rough surface on the meter scale in the vicinity of Tycho, and by analogy Copernicus, is strongly suggested quite independently by the radar observations of Pettengill & Henry (1963). In general the lunar surface is quite smooth at radar wavelengths (Evans, 1962). All of this adds up to a picture not at all incompatible with some of the geological details expected by Shoemaker (1962) and others to characterize large impact structures on the Moon. However, some interesting questions come to mind when one considers what geological processes must be involved in order to transform this rough landscape of virtually unaltered rock surfaces into the very smooth, insulated, and darker landscape which characterizes most of the other, presumably more aged, lunar craters. Radiation damage may well be the explanation of the darkening, but what transforms the surface from rough to smooth on a meter scale and how do the fresh rock surfaces become covered with insulating material? Clearly a redistribution process operating over at least 10 meter ranges must characterize the lunar surface. A seemingly simple way out is to assert that dust sedimentation is going on and the rough, fresh, structures are simply

buried in the course of time (Gold, 1955). But, as was discussed in the preceeding section, the longitudinal temperature variations observed just don't seem to be compatible with a widespread unconsolidated dust layer thick enough to bury meter scale roughness making up the surface of a structure with kilometer scale relief. Furthermore, what is the source of this hypothetical dust sedimentation? Cosmic infall doesn*t seem to be sufficient and may well actually result in greater erosion than sedimentation (Shoemaker, private communication). If the source is thought to be the Moon itself then there should be bare, elevated areas providing the sediment to fill in the newly-formed impact craters (ignoring the problem of what really is the hypothetical transport mechanism). Such bare surfaces would appear as large "hot" regions during the lunar nighttime. Yet, clearly no such bare areas exist to any appreciable extent.

There are, in addition, other very serious difficulties to both the cosmic infall notion and the concept of lunar sedimentation involving transportation over distances of tens of kilometers. In particular, the distinct pattern of albedo variation in the mare areas and the small, but apparently real, color differences in the mare areas (Coyne, 1963) seem to reflect local differences in underlying rock. Such differences in surface deposits would be obliterated by any kind of large scale redistribution of surface material. Many of these and other difficulties can be avoided if the weathering, erosion and sedimentation processes on the Moon are imagined to take place <u>in situ</u>, i.e., not involving redistribution over distances greater than, say, about one kilometer in general.

Problems involved in understanding the present structures characteristic of, and geological process operative on, the lunar surface will not be pursued further here. Our intention has been merely to indicate some of the perplexing

geological implications of the anomalous thermal and microwave properties now known to be associated with some if not all rayed craters, and by the general departure of the nighttime cooling curve from the form predicted by simple models.

V CONCLUSIONS

1. The general variation with longitude of nighttime surface temperature on the Moon seems to be definitely incompatible with the presence of a widespread uniform dust layer of meters thickness such as might be thought to originate by cosmic infall or other mechanism. More conductive material apparently is commonly present either on the surface or within a few centimeters of it.

2. No nighttime temperature difference was found between mare and upland areas; the pattern of vertical and/or horizontal inhomogeneity of thermal properties is apparently independent of the major physiographic character of the Moon. This observation appears to rule out any significant net mass transport in the form of fine particles, from the uplands to the mare.

3. Locally there are extensive occurences of more conductive materials overlain by not more than about 1 mm of dust. Two such occurrences are associated with, but are larger than, the rayed craters Tycho and Copernicus. Two other, less prominant, occurrences on mare border areas may - or may not - be related to small rayed craters.

4. The ageing process of the rayed craters not only involves darkening, but a change from "fresh" to insulated surface conditions and, according to the radar observations of Pettengill (1962), a change from a very rough surface to a smooth one on a meter scale. Although the visual darkening effect might be dismissed simply as a radiation damage phenomenon, the smoothing and insulation effects require weathering, erosion, transport, and sedimentation processes to be operative on the present lunar surface at least over a range of, say, 10 meters.

5. The geological processes which transform rough and fresh terrain to

to smooth and insulated terrain must be of local extent, probably less than a kilometer in range and possibly very much less. Accordingly the redistribution processes appear to be bracketed in the .10 to 1 kilometer range.

Acknowledgements

The authors have received important assistance from the Mount Wilson and Palomar Observatories, from the Naval Ordnance Test Station, China Lake, California, and from the White Mountain Research Station of the University of California. We are particularly indebted to Mr. James A. Westphal, Senior Engineer in the Division of Geological Sciences, for the development of the photometer and other equipment and for considerably help in both the collection and interpretation of the observations. Financial support for the research described here was made available under National Aeronautics and Space Administration grant NsG 56-60 and the National Science Foundation grant G-25210.

VI REFERENCES

1. Allen, (1955), "Astrophysical Quantities," Athlone Press, London.

2. Bratt, P., W. Engeler, H. Levinstein, A MacRoe, and J. Peffek, (1961), Infrared Physics, 1, pp. 27.

3. Coyne, C. V., (1963), Astron. J., 68, pp. 49.

4. Evans, J. V. (1962), in "Physics and Astronomy of the Moon," (Z. Kopal, ed.), Academic Press, pp. 429.

5. Dolfus, A. (1962), in "Physics and Astronomy of the Moon," (Z. Kopal, ed.), Academic Press, pp. 429.

6. Geoffrion, A., M. Korner, and W. M. Sinton (1960), Lowell Obs. Bull., 5, 1.

7. Gold, T., (1955), Mon. Not. R. Astr. Soc., 115, pp 585.

8. Harris, L. and P. Fowler, (1961), J. Opt. Soc. Am., 51, pp. 164-167.

9. Jaeger, J. C., (1953), Aust. J. Phys, 6, pp. 10.

10. Lafner, P., (1952), American Mineralogist, 37.

11. Lyons, R. and Burns, [illegible] (1963), Economic Geology [illegible], 58, pp. 294

12. Murray, B. C. and R. L. Wildey, (1963), Astroph. J., 137, pp. 692.

13. Pettengill, G[illegible], and J. C. Henry, (1962). Jour. Geophysical Res., 67, number 12, pp. 488.

14. Pettit, E., (1935), Astrophy. J., 81, pp. 17.

15. Pettit, E., and S. B. Nicholson, (1930), Astrophy. J., 71, pp. 100.

16. Rosse, Lord, (1869), Proc. Roy. Soc., 17, pp. 436.

17. Shoemaker, E. M., (1962), in, "Physics and Astronomy of the Moon," (Z. Kopal, ed.), Academic Press, pp. 283.

18. Shorthill, R. W., and J. M. Saari, (1961), Publ. Astron Soc. Pac., 73, pp. 335. (Abstract Only).

19. Shorthill, R. W., H. C. Borough, and J. M. Conley, (1960) Publ. Astron Soc. Pac., 77, pp. 481.

20. Sinton, W. M., (1955), J. Opt. Soc. Amer., 45, pp. 975.

21. Sinton, W. M., (1960), Lowell Obs. Bull, 5, pp. 23.

22. Sinton, W. M., (1960), Pub. Astron. Soc. Pac., 72, pp. 362,(Abstract Only).

23. Sinton, W. M., (1962), in "Physics and Astronomy of the Moon," (Z. Kopal, ed.), Academic Press, pp. 407.

IV REFERENCES (con't)

24. Sinton, W. M., and J. Strong (1960), Astrophy J., 131, pp. 472.

25. Sinton, W. M., and J. Strong (1960), Astrophy, J., 131, pp. 459.

26. Smith, R. A., F. E. Jones, and R. P. Chasmar, (1957), "The Detection and Measurement of Infrared Radiation," Oxford at the Clarendon Press.

27. Van Diggelen, J., (1960), Recherches Astron de t'obs. d'Utrecht, 14, pp. 114.

28. Very, F. W., (1898), Astrophy J., 8, pp. 199.

29. Westphal, J. A., Murray, B. C., and D. E. Martz, (1963), Applied Optics, 2, (In Press).

30. Wildey, R. L. and N. Polin, "Photoelectric Investigation of Lunar Brightness vs Phase," (In Preparation).